Vol. 642: 117–132, 2020
https://doi.org/10.3354/meps13312

MARINE ECOLOGY PROGRESS SERIES
Mar Ecol Prog Ser

Published May 28

Low growth resilience of subarctic rhodoliths (*Lithothamnion glaciale*) to coastal eutrophication

David Bélanger[1,*], Patrick Gagnon[2]

[1]Department of Biology, Memorial University of Newfoundland, St. John's, NL, A1B 3X9, Canada
[2]Department of Ocean Sciences, Ocean Sciences Centre, Memorial University of Newfoundland, St. John's, NL, A1C 5S7, Canada

ABSTRACT: Eutrophication is one of the most important drivers of change in coastal marine ecosystems worldwide. Given their slow growth, rhodoliths and the biodiverse communities they support are regarded as non-renewable resources threatened by human activity. Consequences of nutrient enrichment on growth and calcification in crustose coralline algae are equivocal, and even more so in cold-water rhodoliths. We paired a 183 d laboratory mesocosm experiment with a 193 d field experiment on Newfoundland (Canada) rhodoliths (*Lithothamnion glaciale*) to test the hypothesis that nutrient (nitrate, ammonia, and phosphate) enrichment and biofouling reduce rhodolith growth. Rhodoliths in the laboratory were exposed to 1 of 3 nutrient concentrations (ambient, intermediate, or high) and either of 2 levels of manual cleaning (cleaned or uncleaned) to control biofouling. We exposed rhodoliths in the field to 1 of 2 nutrient concentrations (ambient or elevated). Eutrophication in the laboratory did not affect biofouling; however, manual cleaning reduced biofouling by ~4 times relative to uncleaned rhodoliths. Rhodoliths grew 2 times slower at elevated than ambient nutrient concentrations, and ~27% more in cleaned than uncleaned rhodoliths at all concentrations. Rhodoliths in the field also grew significantly slower under elevated than ambient phosphate concentrations, but only during the first 6 wk, indicating some capacity for long-term recovery. We conclude that despite some growth resilience to low and infrequent increases in nutrient concentrations, subarctic *L. glaciale* rhodoliths cannot cope with prolonged exposure to modest eutrophication.

KEY WORDS: Rhodoliths · Coralline algae · Marine calcifiers · Eutrophication · Biofouling · Growth · Nutrient enrichment · Mesocosm experiment

1. INTRODUCTION

Eutrophication is one of the most important drivers of change in coastal marine ecosystems worldwide (Andersen & Conley 2009). Fossil fuel emissions, urban wastewaters, industrial effluents, agriculture runoffs, and fish farming produce major anthropogenic inputs of nitrogen (N) and phosphorus (P) to coastal environments (Selman et al. 2008, Conley et al. 2009). N and P often limit ocean primary production, more specifically in their dissolved inorganic forms: nitrate (NO_3^-), ammonia/ammonium (NH_3/NH_4^+), and phosphate (PO_4^{3-}) (Ryther & Dunstan 1971). Higher N and P concentrations can increase primary production, ultimately altering bottom-up forces that trigger important changes in the structure and function of coastal assemblages (Valiela et al. 1997). Typically, in marine systems undergoing eutrophication, rapid growth of benthic algae and epiphytes exceeds the ability of grazers to control them, resulting in gradual replacement of perennial, canopy-forming vegetation (Duarte 1995).

Many studies consider nitrogen as the main limiting nutrient for marine primary producers (Smith 1984, Larned 1998, Blomqvist et al. 2004), yet phos-

*Corresponding author: david.belanger@mun.ca

phorus limitation also occurs, particularly in environments with high N concentration (Krom et al. 1991). Although high concentrations of N, P, or both generally enhance the growth of marine primary producers (Delgado & Lapointe 1994), excessive phosphate can inhibit growth and calcification (Simkiss 1964), as seen in corals (Dunn et al. 2012) and coralline algae (Björk et al. 1995, Belliveau & Paul 2002, Littler et al. 2010). Growth in coralline algae correlates positively with the rate of addition of new layers of calcified tissue (McCoy & Pfister 2014). Few studies in warm-water coral reef environments have examined the effects of nutrient enrichment on growth and calcification of crustose coralline algae (Björk et al. 1995, Belliveau & Paul 2002, Tanaka et al. 2017). These studies have generally concluded that nutrient enrichment does not improve coralline algal growth. For example, Björk et al. (1995) reported a ~45% decrease in growth rate of *Lithophyllum kotschyanum* and a ~24% decrease in coralline algal abundance near sewer outfalls. Whether this conclusion extends to cold-water coralline algae or to species with more complex morphologies remains unknown.

Rhodoliths are non-geniculate, unattached, benthic coralline red algae with highly calcified tissues that grow only a few millimeters per year (Foster 2001). Depending on species and environmental conditions, rhodoliths vary in size, shape, and growth form, ranging from small twig-like thalli to large (>10 cm across) and highly branched ellipsoids (Woelkerling et al. 1993). They occur in all oceans from the low intertidal zone down to the lower photic zone (Riosmena-Rodriguez et al. 2017), accumulating in structurally complex and biologically diverse communities known as rhodolith beds (Foster 2001). Given their slow growth and accumulation rates, most researchers consider rhodoliths to be non-resilient and non-renewable resources threatened by human activity (Nelson 2009, Riosmena-Rodriguez et al. 2017).

Multiple studies report alteration of rhodolith beds by anthropogenic stressors, including eutrophication (Grall & Hall-Spencer 2003, Gabara et al. 2018). In the Northwest Atlantic, the coralline red alga *Lithothamnion glaciale* dominates coralline assemblages at depths of 15 to 25 m (Adey & Hayek 2011). Rhodoliths (*L. glaciale*) and extensive rhodolith beds develop within this depth range, near natural, urbanized, and industrialized areas along the coast of Newfoundland and Labrador, Canada (Gagnon et al. 2012, Millar & Gagnon 2018, Teed et al. in press). This region provides an excellent opportunity to study the vulnerability of subarctic rhodoliths to eutrophication because of (1) predominantly cold-water environments in which these beds develop (Caines & Gagnon 2012, Blain & Gagnon 2013), and (2) general absence of epiphytes on rhodoliths in the Newfoundland beds studied thus far (Gagnon et al. 2012, Adey et al. 2015, Millar & Gagnon 2018).

We paired a 183 d laboratory mesocosm experiment with a 193 d field experiment on Newfoundland rhodoliths (*L. glaciale*) to test the hypothesis that nutrient enrichment (N and P) and biofouling reduce rhodolith growth. This hypothesis stems from (1) the inhibitory effect of phosphate on growth and calcification, as seen in the crustose coralline alga *L. kotschyanum* (Björk et al. 1995), and (2) the expected proliferation of epiphytes — reducing rhodolith access to light and nutrients, and hence photosynthetic activity and growth — as seen in the seagrasses *Thalassia testudinum* and *Zostera marina* (Drake et al. 2003). Rhodoliths in the laboratory experiment experienced different combinations of nutrient concentrations (ambient, intermediate, or high) and manual cleaning of their surface to control biofouling (cleaned or uncleaned). We held rhodoliths in the field experiment in cages and exposed them to ambient or elevated nutrient concentration. In both experiments, (1) rhodoliths experienced natural variation in sea temperature and photoperiod, (2) slow release of an agricultural fertilizer determined the nutrient concentrations, and (3) we compared rhodolith branch elongation to identify individual and interactive effects of nutrient enrichment and biofouling on growth.

2. MATERIALS AND METHODS

2.1. Rhodolith collection and staining

On 30 May and 4 June 2015, divers hand collected 720 spheroidal rhodoliths measuring 40 to 45 mm in diameter (Fig. 1A) haphazardly at ~15 m depth from the middle of a rhodolith bed in St. Philip's (southeastern Newfoundland, Canada; 47.5926° N, 52.8926° W) (see Gagnon et al. 2012 and Millar & Gagnon 2018 for a detailed description of the bed). Rhodoliths were transported in plastic containers filled with seawater to the Ocean Sciences Center (OSC) of Memorial University of Newfoundland and transferred into 180 l glass tanks (n = 2; 360 rhodoliths in each tank) supplied with flow-through seawater pumped in from a depth of ~5 m in adjacent Logy Bay. We exposed rhodoliths in these tanks for 35 d to natural irradiance and photoperiod of indirect sunlight.

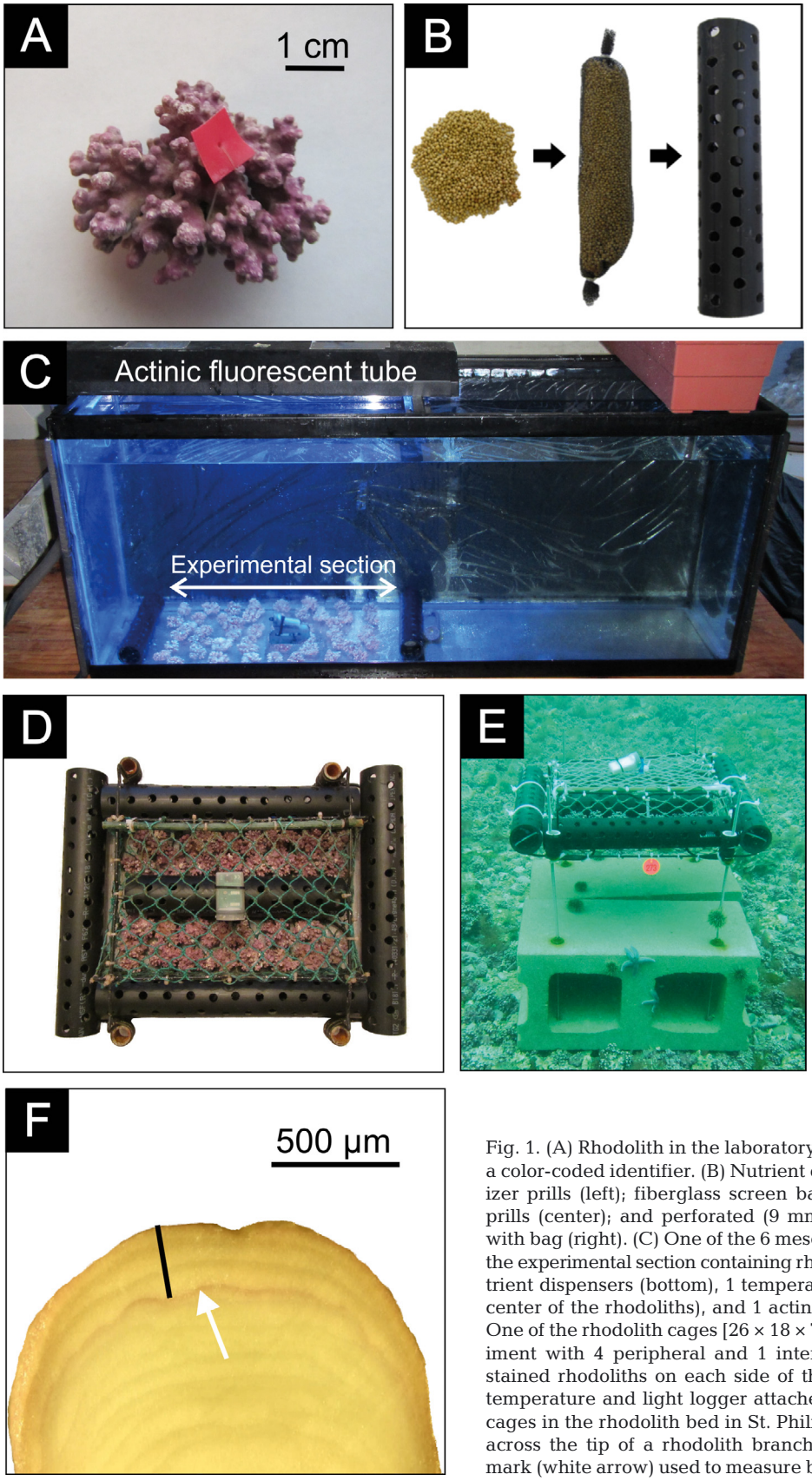

Fig. 1. (A) Rhodolith in the laboratory mesocosm experiment with a color-coded identifier. (B) Nutrient dispenser: Osmocote® fertilizer prills (left); fiberglass screen bag (1.5 mm mesh size) with prills (center); and perforated (9 mm diameter holes) ABS pipe with bag (right). (C) One of the 6 mesocosms (180 l) with location of the experimental section containing rhodoliths, two 25 cm long nutrient dispensers (bottom), 1 temperature and light logger (in the center of the rhodoliths), and 1 actinic fluorescent tube (top). (D) One of the rhodolith cages [26 × 18 × 7 cm] used in the field experiment with 4 peripheral and 1 internal nutrient dispensers, 30 stained rhodoliths on each side of the internal dispenser, and 1 temperature and light logger attached to the top. (E) One of the cages in the rhodolith bed in St. Philip's. (F) Longitudinal section across the tip of a rhodolith branch showing the Alizarin stain mark (white arrow) used to measure branch elongation (black bar)

From 26 to 28 June 2015, we inspected each rhodolith and removed all cryptofauna and epiphytes with forceps and a smooth nylon brush in preparation for rhodolith staining. On 29 June 2015, we stopped seawater delivery to each tank and lowered the water volume to 90 l prior to adding 10 l of seawater containing 8.5 g of dissolved Alizarin Red S (a biological stain commonly used to stain rhodoliths; Riosmena-Rodriguez et al. 2017), yielding a concentration of ~85 mg Alizarin l^{-1}. We held rhodoliths for 48 h in the staining solution at ~6°C with immersion probe coolers (IP-35RCL; PolyScience) controlled by timers. During staining, we aerated each tank with a pump (Elite802; Rolf C. Hagen) that delivered 1500 cm^3 of air min^{-1} to prevent deoxygenation and acidification. Two 61 cm long, actinic fluorescent tubes (Marine-GLO, T8, 20W; Rolf C. Hagen) located ~50 cm above the water surface (1 tube per half section of the tank) emitted light daily from 06:00 to 20:00 h to reflect a natural photoperiod. These actinic tubes, designed to emulate shallow marine coastal light conditions, emitted predominantly in the lower photosynthetically active radiation (PAR) range (400–580 nm). After staining, we reinstated water flow in the tanks, gradually flushing the staining solution.

2.2. Nutrient release

Marine ecologists use slow-release agricultural fertilizers to simulate and study the impacts of nutrient enrichment on plant growth and community structure (Worm et al. 2000). These fertilizers simulate nutrient composition of terrestrial water runoffs and outfalls, while enabling long-term *in situ* enrichment experiments through gradual release of nutrients over time. In both the laboratory mesocosm enrichment experiment (Section 2.3) and the field enrichment experiment (Section 2.4), we used slow-release fertilizer prills (Osmocote® Classic, 19-6-12; Everris) containing 10% ammoniacal nitrogen (NH_3-N), 9% nitrate nitrogen (NO_3-N), 6% phosphorus pentoxide (P_2O_5), and 12% potassium oxide (K_2O). In each experiment, we used custom-built nutrient dispensers to establish the desired nutrient concentrations. Each dispenser consisted of a cylindrical fiberglass screen bag (mesh size = 1.5 mm) filled with fertilizer prills and placed in a perforated (9 mm diameter holes, 13 holes dm^{-2}) ABS pipe (diameter = 3.8 cm) (Fig. 1B). Dispenser size was constrained by mesocosm width and inner-cage length (25 cm, 76 holes), and outer-cage perimeter (30 cm, 92 holes) (Fig. 1B). We carried out pre-experimental trials to study patterns of nutrient release (see Fig. S1, Methods S1, in Supplement 1 at www.int-res.com/articles/suppl/m642p117_supp.pdf) and create repeatable patterns with detectable levels of nitrate, ammonia, and phosphorus in our experiments.

2.3. Mesocosm enrichment experiment

To test individual and interactive effects of nutrient enrichment and biofouling on rhodolith growth, we exposed stained rhodoliths in a 183 d laboratory mesocosm experiment, in a fully crossed design, to 1 of 6 combinations of nutrient concentrations (ambient, intermediate, and high) and biofoulers of rhodolith surfaces (cleaned and uncleaned). We measured the thickness of new layers of tissue added at the tip of branches since marking (see Section 2.6 for details of branch elongation measurement).

The experiment used 180 l glass mesocosms (120 cm long × 30 cm wide × 50 cm deep; n = 6) with flow-through ambient seawater (1 l min^{-1}). We assigned each mesocosm 1 of 2 replicates for each of the 3 nutrient concentrations. Experimental manipulations were carried out in the half section of each mesocosm opposite the seawater inflow to limit rhodolith exposure to non-enriched ambient water input. One 61 cm long, actinic fluorescent tube (Marine-GLO, T8, 20W; Rolf C. Hagen), located ~10 cm above the water surface and emitting ~15 µmol photons m^{-2} s^{-1} of PAR, lit this section of the mesocosms, hereafter the 'experimental section' (Fig. 1C). Electrical timers controlled light emission, adjusted to natural photoperiod throughout the experiment. Opaque canvas on the sides of each mesocosm blocked sunlight coming through the laboratory windows, making actinic light the only significant source of irradiance. We achieved desired nutrient concentrations by placing 1 nutrient dispenser (Fig. 1B) at each end of the experimental section. Mesocosm dispensers for ambient, intermediate, and high nutrient concentrations were filled with respectively 0, 125, or 250 g of fertilizer equally divided between the 2 dispensers in each mesocosm.

On 3 July 2015 (onset of experiment), we placed 2 groups of 30 stained rhodoliths on the bottom of each mesocosm. A small (1 × 1 cm) colored plastic tag affixed to each rhodolith with fishing line (Fig. 1A) provided a unique identifier between 'Cleaned' and 'Uncleaned' rhodolith groups in each mesocosm. Every ~14 d, we transferred all 60 individuals from each mesocosm into a bucket filled with water from their mesocosm, and gently scrubbed rhodoliths in the 'Cleaned' treatment with a smooth nylon brush to remove surface biofoulers; individuals in the 'Un-

cleaned' treatment were left untouched. Rhodoliths were then haphazardly redistributed homogeneously within their mesocosms.

We removed 5 cleaned and 5 uncleaned rhodoliths from each mesocosm on each collection date (Table 1) to measure the biomass of biofoulers growing on rhodoliths and rhodolith branch elongation. The latter collection marked the end of the experiment. We introduced 10 live, unstained 'replacement rhodoliths' to the bottom of each mesocosm after each of the 6 collection events to maintain constant rhodolith density throughout the experiment.

Replacing nutrient dispensers every 3 to 5 wk during the experiment maintained consistently higher nutrient concentrations in the intermediate and high concentration treatments (see Section 2.2). Nutrient concentrations were monitored by collecting water samples every ~7 d from each mesocosm (see Section 2.7). A temperature and light logger (HOBO Pendant; Onset Computer) placed in the center of the experimental section, with the light sensor facing the water surface (Fig. 1C) recorded water temperature and downwelling illuminance every 5 min. We converted illuminance to PAR using:

$$\mathrm{PAR} = \frac{I}{\mathrm{CF}} \quad (1)$$

where PAR is photosynthetically active radiation in µmol photons m^{-2} s^{-1}, I is illuminance in lux (lx), and CF is a lux to PAR conversion factor for high irradiance of 22 lx / µmol photons m^{-2} s^{-1} obtained from simultaneous measurement of illuminance and irradiance for artificial actinic light in the mesocosms (see details of actinic light PAR conversion factor in Table S1, Methods S2, Supplement 2). We calculated daily light integral (DLI), the total amount of photosynthetically active photons received by a given surface over 24 h, for each day and mesocosm using:

$$\mathrm{DLI} = \sum_{i=1}^{288} \frac{300 x_i}{10^6} \quad (2)$$

where DLI is daily light integral in mol photons m^{-2} d^{-1}, 288 is the number of PAR readings over 24 h, x_i is the ith PAR value in µmol photons m^{-2} s^{-1}, 300 is the number of seconds separating 2 consecutive readings (1 reading every 5 min), and 10^6 is the µmol to mol scaling factor.

2.4. Field nutrient enrichment

To test rhodolith responses to nutrient enrichment in a natural habitat, we ran a 193 d experiment at 16 m depth in the rhodolith bed in St. Philip's, monitoring biofouling and growth of stained rhodoliths exposed to ambient or elevated nutrient concentration. Rhodoliths (n = 360) were held in 12 rectangular cages (26 cm long × 18 cm wide × 7 cm deep) made of a metal frame covered in tightly stretched nylon netting with 2 cm mesh (Fig. 1D). We exposed rhodoliths in those cages to either ambient or elevated nutrient concentrations. Four 30 cm long nutrient dispensers surrounded each cage, with an additional 25 cm long central dispenser inside each cage (Fig. 1D). Ambient treatments contained dispensers with no fertilizer prills. The 30 and 25 cm long dispensers in the enriched treatment contained 250 and 200 g of prills, respectively, for a total of 1200 g of fertilizer per cage. We based this quantity (~5 times the amount of fertilizer in the high concentration treatment of the laboratory experiment) on pre-experimental determination of nutrient concentration in water samples taken from cages containing various amounts of fertilizer. Metal rods attached to each corner of the cage and secured to cinder blocks raised cages ~35 cm above the seabed to limit access by benthic grazers such as urchins, chitons, and gastropods (Fig. 1E). Separating cages by at least ~5 m limited nutrient contamination among cages. Ambient and enriched treatments were randomly assigned to cages.

The experiment began on 3 July 2015, when we removed stained rhodoliths from the flow-through mesocosms at the OSC and transported them to the rhodolith bed in 70 l plastic containers filled with seawater. Divers introduced 15 rhodoliths to each preassembled cage on each side of the internal

Table 1. Rhodolith collection dates for the laboratory mesocosm enrichment experiment and the field nutrient enrichment

Experiment	Collection	Date	Days since onset of experiment
Mesocosm	1	31 Jul 2015	29
	2	1 Sep 2015	61
	3	1 Oct 2015	91
	4	1 Nov 2015	122
	5	1 Dec 2015	152
	6	1 Jan 2016 (end of experiment)	183
Field	1	10 Aug 2015	39
	2	4 Sep 2015	64
	3	5 Oct 2015	95
	4	4 Nov 2015	125
	5	3 Dec 2015	154
	6	11 Jan 2016 (end of experiment)	193

nutrient dispenser (for a total of 30 rhodoliths cage^{-1}). This arrangement resulted in similar light and nutrients for each rhodolith. Approximately every month thereafter, divers removed 5 rhodoliths from each cage to measure biofouling and rhodolith growth (Table 1).

We collected 2 water samples from each cage twice monthly to monitor nutrient concentrations (immediately before, and ~15 d after replacing the nutrient dispensers). Two temperature and light loggers (HOBO Pendant; Onset Computer) attached to different cages, with the light sensor facing the sea surface, recorded sea temperature and downwelling illuminance every 5 min throughout the experiment. Illuminance was converted to PAR with Eq. (1), using a conversion factor of 23.5 lx / µmol photons m^{-2} s^{-1} obtained from simultaneous measurement of illuminance and irradiance of sunlight at a depth of 15 m in the rhodolith bed (see sunlight PAR conversion factor details in Table S2, Methods S2, Supplement 2). We calculated DLI for each of the 193 d of the field experiment with Eq. (2).

2.5. Biofouling

We measured the amount of biofoulers on rhodoliths after each of the 6 collections in the laboratory and field experiments. For each collection, we oven-dried rhodoliths at 40°C for 48 h and weighed individuals to obtain rhodolith gross dry weight (W_g). We subsequently scrubbed each rhodolith with a smooth nylon brush to remove all biofoulers and weighed again, yielding rhodolith net dry weight (W_n). We calculated the relative weight of biofoulers for each rhodolith using:

$$\mathrm{R}W_b = \frac{W_g - W_n}{W_n} \quad (3)$$

where $\mathrm{R}W_b$ is the relative dry weight of biofoulers for each rhodolith in mg of biofoulers per g of rhodolith, W_g is the gross dry weight of a given rhodolith in mg, and W_n is the net dry weight of the same rhodolith, also in mg.

2.6. Rhodolith branch elongation

Following oven drying of laboratory and field rhodoliths, we haphazardly chose 5 branches per rhodolith and filed them longitudinally to their center with a rotary tool (3000; Dremel) fitted with a 240-grit sanding disc. Filed branch tips were then hand-polished with a 600-grit sandpaper to expose stain marks and photographed at 40× magnification with a microscope equipped with a digital camera (BA300; Motic). Digital photographs and image analysis software (Motic Images Plus 2.0; Motic) provided measurements of branch elongation, defined as the maximum length of the axis perpendicularly joining the stain mark and apex of the tip (Fig. 1F). We averaged the 5 growth measurements from each rhodolith.

2.7. Water sampling and nutrient analysis

On days of collection, divers transported 12 syringes in a sealed, plastic bag to the rhodolith cages, and slowly approached each cage to avoid stirring up sediment. They removed a syringe from the bag, inserted it in the cage through the netting, completely filled it with water from ~1 cm above the rhodoliths, capped it, and placed it back inside the sealed bag to minimize the risk of contamination with surrounding water. Upon surfacing, 40 ml of water from each syringe were transferred into a 50 ml polypropylene centrifuge tube, placed on ice in a cooler, and transported to the OSC for storage at –20°C.

We measured concentrations of nitrate (NO_3^-), total ammonia (NH_3), and phosphate (PO_4^{3-}) in water samples with a continuous flow autoanalyzer (AA3 HR; Seal Analytical). Frozen samples were thawed in a refrigerator and filtered with 0.7 µm borosilicate glass microfiber filters (Whatman GF/F; GE Healthcare's Life Sciences). We presoaked all materials used for water sample collection and nutrient analysis in a 10% hydrochloride solution for 24 h before rinsing them 3 times with deionized water, and air drying.

2.8. Statistical analysis

We used ANCOVA (Sokal & Rohlf 2012) to examine differences in rates of change of rhodolith branch elongation among our various experimental treatments. Although we measured branch elongation in rhodoliths collected at various time intervals, interpreting statistical differences among regression slopes of experimental treatments effectively compared differences in rhodolith branch elongation rates among treatments (Quinn & Keough 2002). As detailed below, we applied linear mixed-effects models (LMEMs) to various ANCOVA designs with both fixed and random factors to properly handle the dependency

structure of the data and account for pseudoreplication (Zuur et al. 2009).

2.8.1. Laboratory mesocosm experiment

Two LMEMs applied to split-plot ANCOVA experimental designs (Quinn & Keough 2002), with concentration (ambient, intermediate, or high) as a fixed, between-plots factor, mesocosm (each of the 6 experimental mesocosms) as a random factor nested within concentration, biofouling (cleaned or uncleaned rhodoliths) as a fixed, within-plots factor, and covariate time (days elapsed since the onset of the experiment), compared the following: (1) rhodolith biofouling; and (2) rhodolith branch elongation rate among the 6 experimental treatments (n = 360 for each analysis). For each model, we implemented a specific variance structure to satisfy the assumption of homogeneity of variance; an identity variance (varIdent) structure for the first analysis accounted for the lower variance in the abundance of biofoulers on cleaned than uncleaned rhodoliths, and a power of the variance covariate (varPower) structure for the second analysis accounted for increasing variance in rhodolith branch elongation over time (Zuur et al. 2009).

2.8.2. Field experiment

We applied 2 LMEMs to nested ANCOVA experimental designs with concentration (ambient or elevated concentrations) as a fixed factor, cage (each of the 12 cages) as a random factor nested within concentration (6 cages per nutrient concentration), and time (days elapsed since the onset of the experiment) as covariate to test the effect of nutrient concentration on the following: (1) biofouling of rhodoliths; and (2) rhodolith branch elongation rate (n = 360 for each analysis). We implemented a power of the variance covariate (varPower) structure for each model for the same reason explained above.

For all analyses, we verified homogeneity of variance and normality of residuals by examining the distribution of the residuals and the normal probability plot of the residuals, respectively (Snedecor & Cochran 1989). Paired *t*-test comparisons detected differences among levels within a factor (ANCOVAs). All analyses were carried out with R 3.6.1 (R Core Team 2017), using a significance level of 0.05. Rhodolith annual growth reported for the laboratory and field experiments describes model predicted values at time = 365 d (number of days in 1 yr), assuming no growth at the onset of experiment (i.e. intercept corrected to 0).

3. RESULTS

3.1. Laboratory mesocosm experiment

3.1.1. Temperature and light environment

As expected, daily mean water temperature (DMWT) in the mesocosms during the 183 d laboratory experiment varied seasonally, increasing from 10.6 ± 0.2°C (SD) at the onset (3 July 2015) to a maximum of 15.3 ± 0.2°C 53 d later (24 August 2015), and then declined steadily afterwards to a minimum of 2.6 ± 0.2°C at the end (1 January 2016) (Fig. 2A). Contrary to DMWT, DLI in the mesocosms averaged 0.46 ± 0.14 mol photons m^{-2} d^{-1} and was relatively stable throughout the experiment (no seasonal variation), ranging between 0.21 ± 0.07 and 0.81 ± 0.03 mol photons m^{-2} d^{-1} (Fig. 2C). Our modifications to daily lighting in the mesocosms to track the declining photoperiod resulted in a ~75% decrease in mean DLI over the course of the experiment (Fig. 2C).

3.1.2. Nutrients

Compared to the ambient treatment (no fertilizer added), nutrient concentration in the intermediate (125 g of fertilizer) and high (250 g) enrichment treatments was ~3 and 9 times higher for nitrate, respectively; 4 and 10 times higher for ammonia; and 2 and 5 times higher for phosphate (Table S3, Supplement 3). Differences in mean nitrate, ammonia, and phosphate concentrations between the intermediate and high enrichment treatments (Table S3, Supplement 3) largely resulted from sudden increases to peak concentrations in the high enrichment treatment following replacement of the nutrient dispensers (Fig. 3A–C). Nitrate concentration in between peaks was similar in the intermediate and high enrichment treatments, but less so for ammonia and phosphate, which were lower in the high than in the intermediate treatment (Fig. 3A–C). Concentration peaks in the intermediate and high enrichment treatments of the laboratory experiment were ~1 to 2, and 3 to 4 times higher, respectively, than those in pre-experiment trials for corresponding treatments (Fig. 3A–C and see Fig. S1, Methods S1, in Supplement 1).

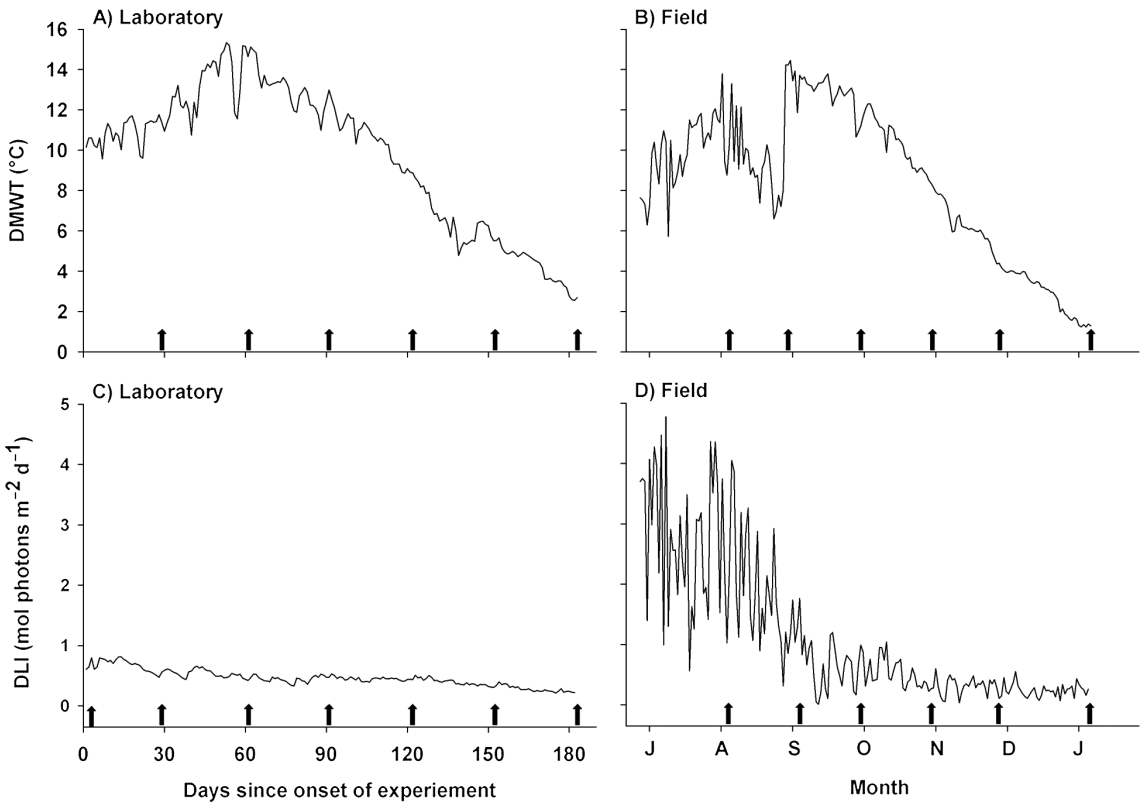

Fig. 2. Daily mean water temperature (DMWT) and daily light integral (DLI) in (A,C) the mesocosms (temperature and irradiance averaged over the 6 mesocosms: 2 for each of the ambient, intermediate, and high nutrient concentration treatments) throughout the 183 d laboratory experiment, and (B,D) at a depth of 16 m in the rhodolith bed throughout the 193 d field experiment. Arrows along abscissas mark days since the onset of the laboratory or field experiments on which 10 laboratory (5 per fouling treatment) or 5 field rhodoliths were removed from each mesocosm or cage to measure biofouling and branch elongation (see Table 1 for collection dates)

3.1.3. Biofouling

Rhodolith biofoulers in the laboratory (and field) experiment consisted primarily of a thin brownish microalgal film, filamentous green and red algae, and bryozoans. Technical considerations prevented finer taxonomic identification. Relative dry weight of biofoulers did not differ significantly among the 3 nutrient concentration treatments, which did not change over time (Table S4, Supplement 3). Nonetheless, biofouler biomass differed significantly and was nearly 4 times greater in uncleaned (0.78 ± 0.12 [CI] mg biofoulers [g rhodolith]$^{-1}$) than cleaned rhodoliths (0.20 ± 0.04 mg) (Table S4, Supplement 3; Fig. 4A).

3.1.4. Rhodolith growth

Rate of change in rhodolith branch elongation differed significantly among the 3 nutrient concentration treatments, with growth rates approximately 2 times higher at ambient concentrations than at intermediate and high concentrations (Table 2; Table S5 in Supplement 3). Mean branch tip elongation at the end of the experiment (after 183 d) was ~2 (high concentration) to 3 (ambient) times higher than measured initially (after 29 d) (Fig. 5A). Resulting annual rhodolith growth rates were nearly twice as high under ambient (398 ± 25 [CI] µm yr^{-1}) than intermediate (230 ± 25 µm yr^{-1}) or high (208 ± 25 µm yr^{-1}) nutrient concentrations (Fig. 6A). Rates of change in branch elongation and associated annual growth rates were ~27 % higher in cleaned (314 ± 23 µm yr^{-1}) than uncleaned (248 ± 23 µm yr^{-1}) rhodoliths in all 3 nutrient concentrations (Table 2; Table S5 in Supplement 3; Figs. 5B & 6B).

3.2. Field experiment

3.2.1. Temperature and light environment

Seasonal variation in DMWT in the rhodolith bed during the 193 d field experiment paralleled the lab-

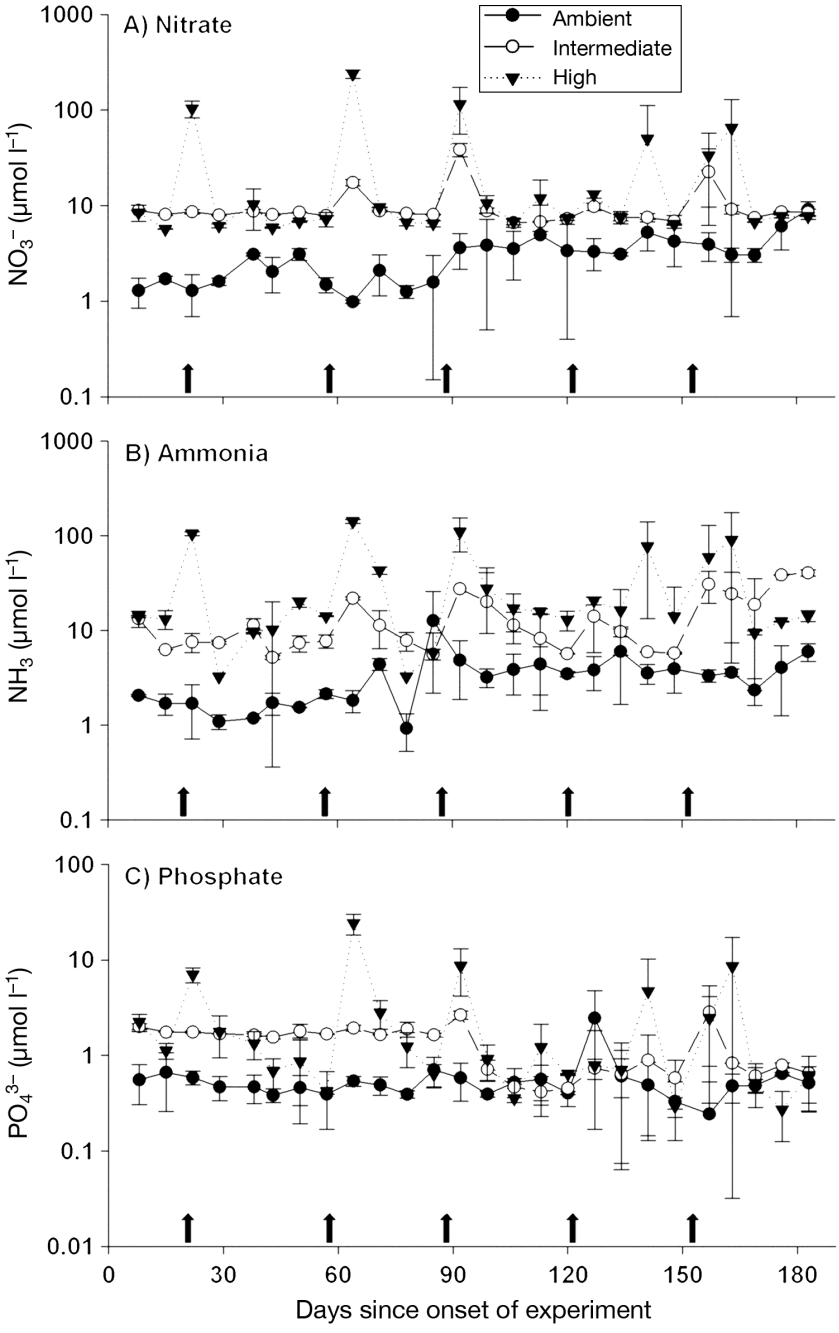

Fig. 3. Mean (±SD) concentration of (A) nitrate (NO_3^-), (B) ammonia (NH_3), and (C) phosphate (PO_4^{3-}) for each nutrient concentration treatment (ambient, intermediate, and high) for each of the 26 water collections during the 183 d laboratory mesocosm experiment. Each concentration is the average from the 2 mesocosms per concentration treatment. Note the change in scale along the (log-scaled) ordinates. Arrows along the abscissas in all panels mark days since the onset of the experiment on which nutrient dispensers were replaced with new ones: Day 20 (22 Jul 2015), 57 (28 Aug 2015), 88 (28 Sep 2015), 121 (31 Oct 2015), and 153 (2 Dec 2015)

oratory experiment, increasing from 7.6 ± 0.9°C at the onset (3 July 2015) to a maximum of 14.5 ± 0.7°C during the first week of September, and then declining to a minimum of 1.2 ± 0.1°C near the end (11 January 2016) (Fig. 2B). The thermocline position during summer overlapped the experimental depth (16 m), causing larger variation in DMWT during the first 2 mo than in the laboratory experiment, including relatively sudden changes of up to ~6°C over 24 h (Fig. 2B). Mean DMWT during the field experiment was 8.4 ± 3.7°C. Contrary to the laboratory experiment, DLI in the rhodolith bed varied strongly seasonally, peaking at 4.78 mol photons m^{-2} d^{-1} and averaging 2.52 ± 1.11 mol photons m^{-2} s^{-1} from July to August, before declining by 80% from September to January to values as low as 0.46 ± 0.34 mol photons m^{-2} s^{-1}, i.e. similar to mean DLI in the laboratory mesocom experiment (Fig. 2D). Mean DLI during the field experiment, 1.10 ± 1.17 mol photons m^{-2} s^{-1}, was 2 times higher than mean DLI during the laboratory experiment.

3.2.2. Nutrients

Mean concentrations of nitrate, ammonia, and phosphate during the experiment were ~1.5, 1.5, and 2 times higher, respectively, in the elevated (250 g of fertilizer added) than ambient (no fertilizer added) treatments (Table S3, Supplement 3). Nutrient concentration was lower for the ambient cages than in elevated concentration treatments on the 12 collection dates (Fig. 7A–C). Nitrate in the ambient treatment remained low, ~0.21 ± 0.11 µmol l^{-1}, from July to early November, when it increased by 1 order of magnitude and further increased to a maximum of 3.92 ± 0.36 µmol l^{-1} at the end of the experiment, on 11 January (Fig. 7A). Nitrate in the elevated treatment exhibited a similar pattern, only with higher concentrations. Ammonia varied considerably in both treatments throughout the experiment, ranging from 0.88 ± 0.47 µmol l^{-1} on 14 September (ambient) to 8.79 ± 2.55 µmol l^{-1} on 13 October (elevated) (Fig. 7B). Phosphate remained fairly low and stable throughout the experiment, peaking

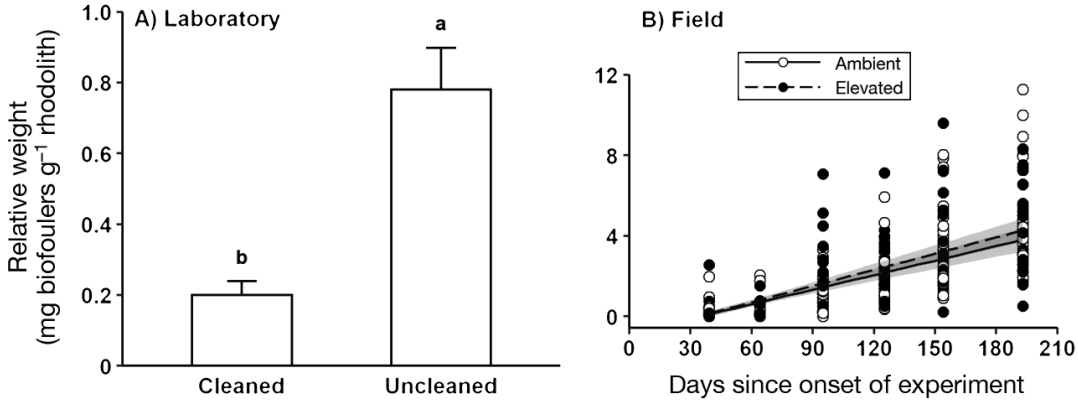

Fig. 4. (A) Relative dry weight (+95% CI) of biofoulers on rhodoliths for each level of rhodolith cleaning (cleaned and uncleaned; pooled over nutrient concentration treatments) in the laboratory mesocosm experiment. Bars not sharing the same letter differ statistically (least-squares means test, $p < 0.05$; n = 36 for each level of cleaning). (B) Increase in relative dry weight (±95% CI) of biofoulers throughout the field experiment for each nutrient concentration treatment (ambient and elevated). See Table 1 for collection dates and Table 2 for details of coefficients of regression slopes presented in panel (B)

Table 2. Summary of regression coefficients of the 2 split-plot ANCOVAs in the laboratory experiment, and 2 nested ANCOVAs in the field experiment (applied to raw data) examining the relationships between relative dry weight of biofoulers on rhodoliths or rhodolith branch elongation, and time elapsed since the onset of the 183 d laboratory mesocosm and 193 d field experiments at the various nutrient concentrations and levels of manual cleaning of rhodoliths (biofouling) tested

Experiment/ response variable	Factor/level	N	Intercept (SE)	Slope (SE)
Laboratory/ relative dry weight of biofoulers	Concentration			
	Ambient	120	0.49 (0.13)	0.000 (0.001)
	Intermediate	120	0.34 (0.13)	0.001 (0.001)
	High	120	0.40 (0.13)	0.001 (0.001)
	Biofouling			
	Cleaned	180	0.20 (0.02)	0.000 (0.000)
	Uncleaned	180	0.78 (0.06)	0.002 (0.001)
Laboratory/ rhodolith growth	Concentration			
	Ambient	120	69.6 (3.6)	1.086 (0.043)
	Intermediate	120	87.9 (3.6)	0.644 (0.043)
	High	120	90.4 (3.6)	0.567 (0.043)
	Biofouling			
	Cleaned	180	78.3 (4.2)	0.855 (0.038)
	Uncleaned	180	86.6 (3.9)	0.679 (0.038)
Field/ relative dry weight of biofoulers	Concentration			
	Ambient	180	−0.84 (0.13)	0.024 (0.002)
	Elevated	180	−0.91 (0.13)	0.027 (0.002)
Field/ rhodolith growth	Concentration			
	Ambient	180	118.6 (7.2)	1.272 (0.085)
	Elevated	180	99.7 (6.9)	1.313 (0.085)

to 0.52 ± 0.18 (ambient) and 1.70 ± 0.15 (elevated) µmol l^{-1} on 31 August (Fig. 7C). Mean nutrient concentrations in the field were up to 9 times lower than those in the intermediate and high nutrient concentration treatments in the laboratory experiment (Table S3, Supplement 3).

3.2.3. Biofouling

Relative dry weight of rhodolith biofoulers did not differ significantly between the ambient and elevated nutrient concentration treatments (Table S6, Supplement 3). It consistently increased, at an average rate of 0.03 ± 0.00 (CI) mg biofoulers (g rhodoliths)$^{-1}$ d^{-1}, from 0.23 ± 0.02 mg on the first collection (10 August), to 4.71 ± 0.34 mg biofoulers (g rhodoliths)$^{-1}$ at the end of experiment (11 January) (Table S6, Supplement 3; Fig. 4B). At the end of the experiment, relative dry weight of rhodolith biofoulers was ~24 and 6 times higher than at the start for the cleaned and uncleaned rhodoliths in the laboratory experiment, respectively (Fig.4A,B).

3.2.4. Rhodolith growth

Branch elongation was significantly lower in rhodoliths exposed to elevated than ambient nutrient concentrations during the 39 d separating the onset of the field experiment and the first rhodolith collection (Table S7, Supplement 3; Fig. 5C). Growth then stabilized for the

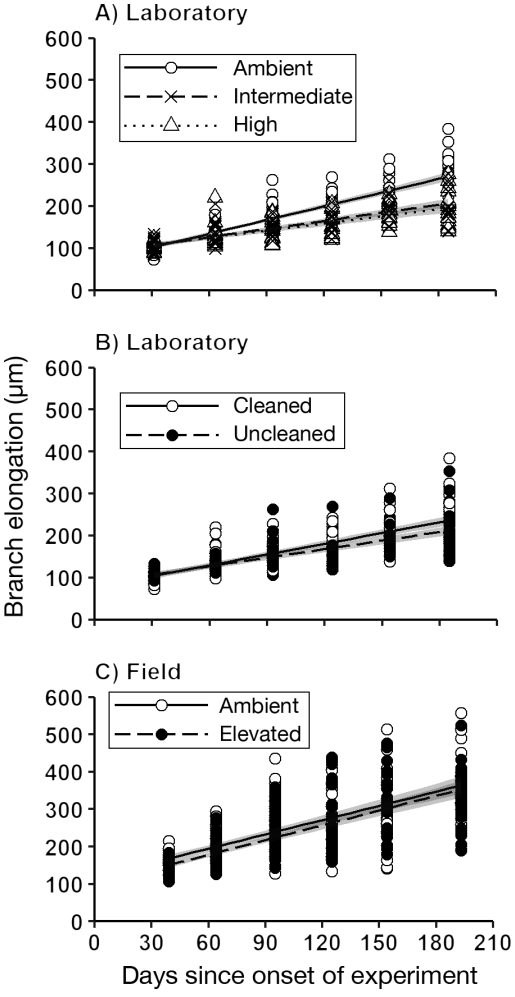

Fig. 5. Branch elongation (±95% CI) of rhodoliths over time: (A) for 3 nutrient concentration treatments (ambient, intermediate, and high; pooled over rhodolith cleaning treatments) in the laboratory mesocosm experiment; (B) for 2 levels of rhodolith cleaning (cleaned and uncleaned; pooled over nutrient concentration treatments) in the laboratory mesocosm experiment; and (C) for 2 nutrient concentration treatments (ambient and elevated) in the field experiment. See Table 1 for collection dates and Table 2 for details of coefficients of regression slopes presented in all panels

remainder of the experiment, increasing at similar rates of 460 ± 51 (CI) and 482 ± 50 µm yr^{-1} in the ambient and elevated treatments, respectively (Table S7, Supplement 3; Figs. 5C & 6C). Mean branch elongation rate in the field was ~18% higher than the ambient nutrient concentration treatment of the laboratory experiment, and about 2 times higher than the intermediate and high concentration treatments (Fig. 6A,C).

4. DISCUSSION

The laboratory mesocosm and field experiments showed that biofouling and elevated nutrient concentration can reduce branch elongation in *Lithothamnion glaciale* rhodoliths. In the laboratory, growth in rhodoliths exposed for 6 mo to nutrient concentrations between ~2 (phosphate; PO_4^{3-}) and 9 (ammonia; NH_3) times higher than the ambient concentrations, decreased by ~46%. Yet, in the field, nutrient concentrations between ~1 (ammonia) and 3

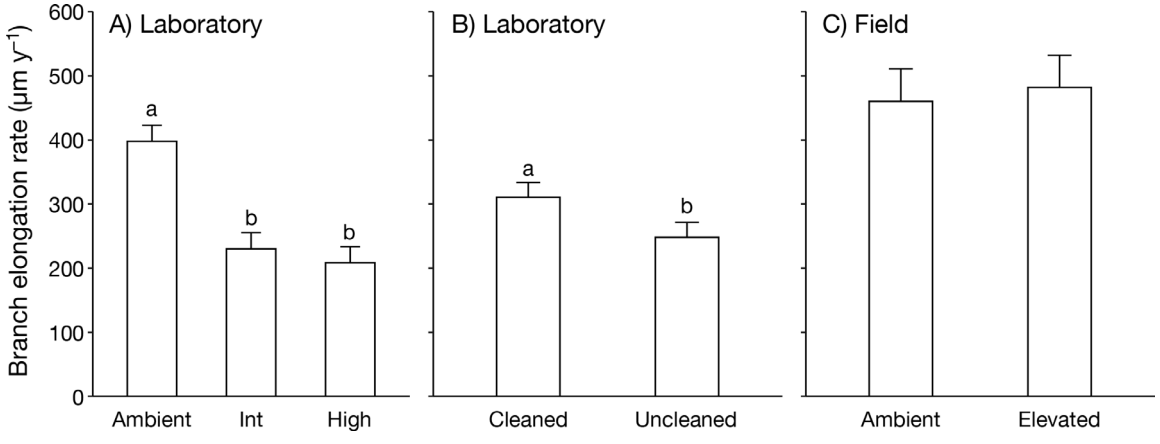

Fig. 6. Mean (+95% CI) annual branch elongation rate of rhodoliths: (A) for 3 nutrient concentration treatments (ambient, intermediate, and high; pooled over rhodolith cleaning treatments) in the laboratory mesocosm experiment; (B) for 2 levels of rhodolith cleaning (cleaned and uncleaned; pooled over nutrient concentration treatments) in the laboratory mesocosm experiment; and (C) for 2 nutrient concentration treatments (ambient and elevated) in the field experiment. Annual growth rates were calculated from the slopes of the linear regressions (presented in Table 2). Bars not sharing the same letter differ statistically (pairwise *t*-test comparisons, $p < 0.05$)

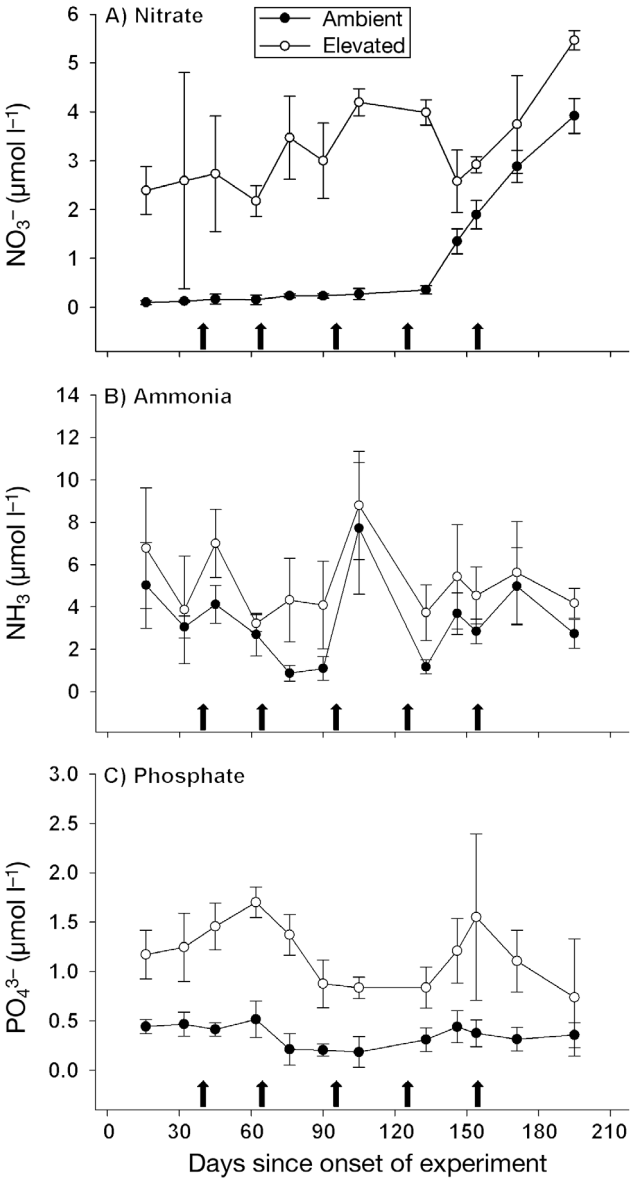

Fig. 7. Mean (±SD) concentration of (A) nitrate (NO_3^-), (B) ammonia (NH_3), and (C) phosphate (PO_4^{3-}) for each nutrient concentration treatment (ambient and enriched) for each of the 12 water collections during the 193 d field experiment. Each concentration is the average from the 6 rhodolith cages per concentration treatment. Arrows along the abscissas in all panels mark days since the onset of the experiment on which nutrient dispensers were replaced with new ones: Day 39 (10 Aug 2015), 64 (4 Sep 2015), 95 (5 Oct 2015), 125 (4 Nov 2015), and 154 (3 Dec 2015)

(nitrate; NO_3^-) times higher than the ambient ones had no effect on growth over 6 mo. Contrary to our expectation, increasing nutrient concentration did not increase biofouling in either experiment. In the laboratory experiment, however, biofouling was ~4 times lower, and growth ~27% higher, in cleaned compared to uncleaned rhodoliths treatments regardless of nutrient concentration.

4.1. Biofouling

In laboratory mesocosms, most rhodolith biofoulers consisted of a thin, brownish microalgal film with a few occasional filamentous algae and bryozoans. Devlin et al. (2007) proposed eutrophication threshold concentrations of dissolved inorganic nitrogen (DIN), including nitrate and ammonia, between 13 and 20 µmol l^{-1} for UK coastal waters. Combined nitrate and ammonia concentrations in the intermediate and high concentration treatments of 88% of water samples from our laboratory experiment were within or above the latter threshold range. The generally lower irradiance in the laboratory mesocosms, particularly during the first ~60 d of the experiment, may have been insufficient to promote continuous growth of epiphytes as seen in the field cages. Admiraal (1976) reported peak growth rates of 4 estuarine benthic diatom species at daily quantum irradiances of 2.5 to 5 mol photons m^{-2} d^{-1}, which are 3 to 6 times higher than the mean irradiance in our mesocosms. The relatively high turnover rate of seawater in our mesocosms presumably limited supply and settlement of spores or larvae of potential biofoulers. Nonetheless, consistently higher biofouling in uncleaned than in cleaned rhodoliths did not prevent rhodolith growth, indicating suitable physical and chemical conditions in the mesocosms to sustain rhodoliths and biofouler recruits.

In the field, a thin film of mainly filamentous algae developed on the surface of rhodoliths. In contrast to the laboratory experiment, biofouling increased consistently over time, with at least 6 times more fouling in field than laboratory rhodoliths by the end of the experiment. Biofouling occurred at a similar rate for rhodoliths exposed to ambient and elevated nutrient concentrations, despite nitrate, ammonia, and phosphate concentrations ~2 to 3 times higher in the elevated treatment. Combined nitrate and ammonia concentrations in the latter treatment, however, still fell below the lower DIN limit of 13 µmol l^{-1} noted above for eutrophication in cold-water systems, except perhaps on those few occasions when we replaced nutrient dispensers with fresh ones and nutrient concentrations increased for a few hours as suggested by the observed nutrient release profiles. Presumably, prolonged exposure to sub-threshold nutrient concentrations prevented increased epiphyte growth. Rasher et al. (2012) observed nutrient-

driven macroalgal blooms in coral reefs only where herbivore grazing was suppressed. These findings suggest that top-down control could be more important than bottom-up processes in controlling macroalgal blooms in eutrophic environments. By raising rhodolith cages above the seabed, we limited grazing by some large grazers (e.g. fish and adult urchins). However, smaller grazers (e.g. gastropods and juvenile urchins) likely entered the cages and offset biofouling in cages with elevated nutrient concentration. Interestingly, Lapointe et al. (1993) reported nitrogen and phosphorus thresholds for bottom-up control of macroalgal growth in tropical coral reefs ~4 times lower than ambient concentrations at our study site, which suggests a greater vulnerability of rhodoliths to eutrophication-induced biofouling in tropical (largely oligotrophic) than polar or temperate (largely eutrophic) systems.

4.2. Rhodolith growth

In the laboratory mesocosm experiment, 27% lower branch elongation of uncleaned rhodoliths than of cleaned rhodoliths represented a considerable difference considering that biofoulers, which were 4 times more abundant on uncleaned rhodoliths, formed only a thin and scattered film on their surface. Irradiance strongly influences growth of *L. glaciale* rhodoliths (Teichert & Freiwald 2014), so that a greater abundance of biofoulers than in our study could block light or reduce nutrient availability, thus further limiting rhodolith growth. Our rhodolith growth rate of ~221 µm yr^{-1} (pooled rate) was also statistically similar between the 2 elevated nutrient concentrations in the laboratory experiment despite phosphate and nitrate concentrations 2 and 3 times higher, respectively, in the high compared to intermediate concentration treatments. Differences in nutrient concentrations between both treatments mostly resulted from higher peaks in the high-concentration treatment shortly after replacing the nutrient dispensers. In between peaks, rhodolith treatments experienced similar concentrations of nitrate, ammonia, and phosphate, which may explain similar rhodolith growth in both treatments.

Previous studies draw mixed conclusions about the effect of elevated nitrogen concentration on growth and calcification in coralline algae. For example, Björk et al. (1995) reported no effect on growth of nitrogen concentrations up to 5 µmol l^{-1} above ambient levels. Johnson & Carpenter (2018) showed a 90 to 130% increase in calcification with elevated nitrate, nitrite, and ammonium concentrations through a significant increase in photosynthetic pigment content. No study reported an inverse relationship between nitrogen concentration and growth or calcification in coralline algae. Nonetheless, Björk et al. (1995) showed a linear decrease in growth with increasing phosphate concentration between ~0.5 and 18 µmol l^{-1}. Their study also reported a ~9 to 33% increase in coralline algal cover with increasing distance from sewer outfalls, with greatest increases at phosphate concentrations <0.3 µmol l^{-1}. Other studies reported significant decreases in coralline algal cover at phosphate concentrations of 0.31 µmol l^{-1} (Belliveau & Paul 2002) and 0.69 to 0.94 µmol l^{-1} (Littler et al. 2010). These phosphate concentrations, measured in naturally oligotrophic coral reef systems, presumably mismatch our more nutrient-rich, temperate coastal systems. In our study, ambient phosphate concentrations in the laboratory and field experiments were 0.6 and 0.4 µmol l^{-1}, respectively, which approaches or exceeds the most detrimental levels reported for oligotrophic systems. In all cases, the negative impact of phosphate on coralline algal growth was likely caused by the inhibitory effect of phosphorus on calcification processes (Simkiss 1964).

The significant decrease in rhodolith growth rates in our laboratory experiment occurred at phosphate concentrations of 1.31 µmol l^{-1} (intermediate enrichment) and 2.88 µmol l^{-1} (high enrichment), comparable to concentrations at the outlet of a heavily drained, subtropical coastal catchment discharging nutrient-laden water into an estuarine system (Santos et al. 2013). Our results compare with those of Schubert et al. (2019), who reported that net photosynthetic performance of Brazilian *Melyvonnea erubescens* rhodoliths decreased significantly at phosphate concentrations of 5.6 µmol l^{-1}. Rhodoliths in our field experiment also grew significantly slower under elevated (1.2 µmol l^{-1}) than ambient (0.4 µmol l^{-1}) phosphate concentrations, but only during the first ~6 wk, after which growth resumed and remained similar between treatments. Apparently, abnormally high phosphate concentrations may impact *L. glaciale* rhodoliths initially, but they have some capacity to recover in the long run. Nutrient release profiles from our pre-experimental trials carried out in laboratory mesocosms suggest that nutrient pulses occurred in the field shortly after we replaced nutrient dispensers, but we could not detect this effect because of the timing of our field sampling. Nutrients dispersed more efficiently in the field cages than in the laboratory mesocosms, as indicated by similar mean levels of enrichment in the field obtained with

a quantity of fertilizer ~10 times higher than in the laboratory. As in the laboratory experiment, we replaced nutrient dispensers in the field experiment 6 times (once every 25 to 39 d), limiting the number of potential nutrient pulses. Most likely, the magnitude and duration of the phosphate pulses in the field cages were less than in the laboratory mesocosms and below the inhibitory threshold for growth in *L. glaciale* rhodoliths. These results confirm those of Tanaka et al. (2017), who reported no effect of phosphate concentrations between 1 and 2 µmol l^{-1} on calcification rates of the coralline red alga *Porolithon onkodes*. Although we did not measure water flow in the field, wave and tidal currents certainly contributed to the greater dispersal of nutrients away from the rhodoliths than in the more stagnant water of the laboratory mesocosms. More research is needed to elucidate the sole effect of water flow on the response of rhodoliths to nutrients. In a follow-up study, we demonstrate the predominant role of irradiance on *L. glaciale* rhodolith growth (Bélanger & Gagnon unpubl. data). In the present study, irradiance in the field was about twice as high as in the laboratory, which may largely explain our observed 15% faster rhodolith branch elongation at ambient nutrient concentration in the field.

4.3. Conclusions and future research directions

Our laboratory experiment supported our overall hypothesis that nutrient enrichment (nitrogen and phosphorus) and biofouling reduce rhodolith (*L. glaciale*) growth, although this was less clear from the field experiment. Contrary to our expectation, elevated concentrations of nitrate and ammonia in the laboratory experiment triggered very little growth of biofoulers on rhodoliths, suggesting that the inhibitory effect of phosphate on (presumably) rhodolith calcification processes primarily explained decreased rhodolith growth in the enriched treatments. Our laboratory experiment clearly demonstrated, and the field experiment suggested, fewer effects of nutrient pulses on rhodolith growth than the relatively stable and lower, yet still elevated, concentrations that prevailed most of the time. These findings indicate some degree of growth resilience (sensu DeSoto et al. 2020) in subarctic *L. glaciale* rhodoliths to modest and infrequent (approximately once a month) increases in nutrient concentrations, yet an inability to cope with prolonged (several months) exposure to slightly eutrophic conditions.

Rhodolith beds are globally distributed, representing a pervasive and important marine biological system (Foster 2001, Riosmena-Rodriguez et al. 2017). As coralline red algae, rhodoliths form an important carbon sink, particularly on temperate and cold-water shelves where they play a significant role in marine carbon cycling (Basso 2012, van der Heijden & Kamenos 2015, Teed et al. in press). Despite the implementation of antipollution laws to reduce the direct discharge of nutrients and toxic substances into coastal waters, anthropogenic inputs of nitrogen and phosphorus in coastal waters have globally increased because of ever-increasing urbanization and industrialization of coastal areas (Small & Nicholls 2003). In subarctic and Arctic regions, ongoing changes in nutrient cycling and freshwater runoff resulting from permafrost thawing and snow melting will likely increase coastal nutrient inputs (Walvoord & Striegl 2007, Kendrick et al. 2018). Our study documents, for the first time, the effects of nutrient enrichment and associated biofouling on growth in *L. glaciale*, a dominant reef-building and rhodolith-forming species in Atlantic subarctic and Arctic marine systems (Adey & Hayek 2011). Like other marine calcifiers, rhodoliths face increasing threats from ocean acidification and warming (Kamenos et al. 2013). Predicting changes in their abundance and the rich biological communities they support requires better understanding of the impacts of nutrient enrichment on rhodolith growth and calcification and their interaction with ocean acidification and warming.

Acknowledgements. We are grateful to A.P. St-Pierre, K. Millar, S. Trueman, D. Frey, and P. Schryburt for help with field and laboratory work; D. Schneider for statistical advice; Gary Maillet, Sandy Fraser, and Gina Doyle for help with nutrient analysis; and J. Wacasey for provision of fertilizer. We also thank P. Snelgrove, R. Gregory, and 3 anonymous reviewers for constructive comments that helped improve the manuscript. This research was supported by Natural Sciences and Engineering Research Council (NSERC- Discovery Grant), Canada Foundation for Innovation (CFI- Leaders Opportunity Funds), Research & Development Corporation of Newfoundland and Labrador (Ignite R&D), and Department of Fisheries and Aquaculture of Newfoundland and Labrador (DFA) grants to P.G.; D.B. was supported by the Memorial University of Newfoundland President's Doctoral Student Investment Fund program.

LITERATURE CITED

Adey W, Hayek LA (2011) Elucidating marine biogeography with macrophytes: Quantitative analysis of the North Atlantic supports the thermogeographic model and demonstrates a distinct subarctic region in the northwestern Atlantic. Northeast Nat 18:1–128

Adey W, Halfar J, Humphreys A, Suskiewicz T, Belanger D, Gagnon P, Fox M (2015) Subarctic rhodolith beds promote longevity of crustose coralline algal buildups and their climate archiving potential. Palaios 30: 281–293

Admiraal W (1976) Influence of light and temperature on the growth rate of estuarine benthic diatoms in culture. Mar Biol 39:1–9

Andersen J, Conley DJ (eds) (2009) Eutrophication in coastal ecosystems: towards better understanding and management strategies. Selected papers from the second international symposium on research and management of eutrophication in coastal ecosystems, 20-23 June 2006, Nyborg, Denmark. Springer, Dordrecht

Basso D (2012) Carbonate production by calcareous red algae and global change. Geodiversitas 34:13–33

Belliveau SA, Paul VJ (2002) Effects of herbivory and nutrients on the early colonization of crustose coralline and fleshy algae. Mar Ecol Prog Ser 232:105–114

Björk M, Mohammed SM, Björklund M, Semesi A (1995) Coralline algae, important coral-reef builders threatened by pollution. Ambio 24:502–505

Blain C, Gagnon P (2013) Interactions between thermal and wave environments mediate intracellular acidity (H_2SO_4), growth, and mortality in the annual brown seaweed *Desmarestia viridis*. J Exp Mar Biol Ecol 440:176–184

Blomqvist S, Gunnars A, Elmgren R (2004) Why the limiting nutrient differs between temperate coastal seas and freshwater lakes: a matter of salt. Limnol Oceanogr 49: 2236–2241

Caines S, Gagnon P (2012) Population dynamics of the invasive bryozoan *Membranipora membranacea* along a 450 km latitudinal range in the subarctic northwestern Atlantic. Mar Biol 159:1817–1832

Conley DJ, Paerl HW, Howarth RW, Boesch DF and others (2009) Controlling eutrophication: nitrogen and phosphorus. Science 323:1014–1015

DeSoto L, Cailleret M, Sterck F, Jansen S and others (2020) Low growth resilience to drought is related to future mortality risk in trees. Nat Commun 11:545

Delgado O, Lapointe B (1994) Nutrient-limited productivity of calcareous versus fleshy macroalgae in a eutrophic, carbonate-rich tropical marine environment. Coral Reefs 13:151–159

Devlin M, Painting S, Best M (2007) Setting nutrient thresholds to support an ecological assessment based on nutrient enrichment, potential primary production and undesirable disturbance. Mar Pollut Bull 55:65–73

Drake LA, Dobbs FC, Zimmerman RC (2003) Effects of epiphyte load on optical properties and photosynthetic potential of the seagrasses *Thalassia testudinum* Banks ex König and *Zostera marina* L. Limnol Oceanogr 48: 456–463

Duarte CM (1995) Submerged aquatic vegetation in relation to different nutrient regimes. Ophelia 41:87–112

Dunn JG, Sammarco PW, Lafleur G (2012) Effects of phosphate on growth and skeletal density in the scleractinian coral *Acropora muricata*: a controlled experimental approach. J Exp Mar Biol Ecol 411:34–44

Foster M (2001) Rhodoliths: between rocks and soft places. J Phycol 37:659–667

Gabara SS, Hamilton SL, Edwards MS, Steller DL (2018) Rhodolith structural loss decreases abundance, diversity, and stability of benthic communities at Santa Catalina Island, CA. Mar Ecol Prog Ser 595:71–88

Gagnon P, Matheson K, Stapleton M (2012) Variation in rhodolith morphology and biogenic potential of newly discovered rhodolith beds in Newfoundland and Labrador (Canada). Bot Mar 55:85–99

Grall J, Hall-Spencer JM (2003) Problems facing maerl conservation in Brittany. Aquat Conserv 13:S55–S64

Johnson MD, Carpenter RC (2018) Nitrogen enrichment offsets direct negative effects of ocean acidification on a reef-building crustose coralline alga. Biol Lett 14: 20180371

Kamenos NA, Burdett HL, Aloisio E, Findlay HS and others (2013) Coralline algal structure is more sensitive to rate, rather than the magnitude, of ocean acidification. Glob Change Biol 19:3621–3628

Kendrick MR, Huryn AD, Bowden WB, Deegan LA and others (2018) Linking permafrost thaw to shifting biogeochemistry and food web resources in an arctic river. Glob Change Biol 24:5738–5750

Krom MD, Kress N, Brenner S, Gordon LI (1991) Phosphorus limitation of primary productivity in the eastern Mediterranean Sea. Limnol Oceanogr 36:424–432

Lapointe BE, Littler MM, Littler DS (1993) Modification of benthic community structure by natural eutrophication: the Belize barrier reef. Proc 7th Int Coral Reef Symp 1: 323–334

Larned ST (1998) Nitrogen-versus phosphorus-limited growth and sources of nutrients for coral reef macroalgae. Mar Biol 132:409–421

Littler MM, Littler DS, Brooks BL (2010) The effects of nitrogen and phosphorus enrichment on algal community development: artificial mini-reefs on the Belize barrier reef sedimentary lagoon. Harmful Algae 9:255–263

McCoy SJ, Pfister CA (2014) Historical comparisons reveal altered competitive interactions in a guild of crustose coralline algae. Ecol Lett 17:475–483

Millar KR, Gagnon P (2018) Mechanisms of stability of rhodolith beds: sedimentological aspects. Mar Ecol Prog Ser 594:65–83

Nelson WA (2009) Calcified macroalgae—critical to coastal ecosystems and vulnerable to change: a review. Mar Freshw Res 60:787–801

Quinn GP, Keough MJ (2002) Experimental design and data analysis for biologists. Cambridge University Press, Cambridge

R Core Team (2017) R: a language and environment for statistical computing. R Foundation for Statistical Computing, Vienna

Rasher DB, Engel S, Bonito V, Fraser GJ, Montoya JP, Hay ME (2012) Effects of herbivory, nutrients, and reef protection on algal proliferation and coral growth on a tropical reef. Oecologia 169:187–198

Riosmena-Rodriguez R, Nelson W, Aguirre J (2017) Rhodolith/maërl beds: a global perspective. Springer International Publishing, Cham

Ryther JH, Dunstan WM (1971) Nitrogen, phosphorus, and eutrophication in the coastal marine environment. Science 171:1008–1013

Santos IR, de Weys J, Tait DR, Eyre BD (2013) The contribution of groundwater discharge to nutrient exports from a coastal catchment: post-flood seepage increases estuarine N/P ratios. Estuaries Coasts 36:56–73

Schubert N, Salazar VW, Rich WA, Vivanco Bercovich M and others (2019) Rhodolith primary and carbonate production in a changing ocean: the interplay of warming and nutrients. Sci Total Environ 676:455–468

Selman M, Greenhalgh S, Diaz R, Sugg Z (2008) Eutrophication and hypoxia in coastal areas: a global assessment of the state of knowledge. World Resources Institute, Washington, DC

Simkiss K (1964) Phosphate as crystal poisons of calcification. Biol Rev Camb Philos Soc 39:487–505

Small C, Nicholls RJ (2003) A global analysis of human settlement in coastal zones. J Coast Res 19:584–599

Smith S (1984) Phosphorus versus nitrogen limitation in the marine environment. Limnol Oceanogr 29:1149–1160

Snedecor GW, Cochran WG (1989) Statistical methods, 8th edn. Iowa State University Press, Ames, IA

Sokal RR, Rohlf FJ (2012) Biometry: the principles and practice of statistics in biological research, 4th edn. W.H. Freeman, New York, NY

Tanaka Y, Suzuki A, Sakai K (2017) Effects of elevated seawater temperature and phosphate enrichment on the crustose coralline alga *Porolithon onkodes* (Rhodophyta). Phycol Res 65:51–57

Teed L, Bélanger D, Gagnon P, Edinger E (in press) Calcium carbonate ($CaCO_3$) production of a subpolar rhodolith bed: methods of estimation, effect of bioturbators, and global comparisons. Estuar Coast Shelf Sci, https://doi.org/10.1016/j.ecss.2020.106822

Teichert S, Freiwald A (2014) Polar coralline algal $CaCO_3$ production rates correspond to intensity and duration of the solar radiation. Biogeosciences 11:833–842

Valiela I, McClelland J, Hauxwell J, Behr PJ, Hersh D, Foreman K (1997) Macroalgal blooms in shallow estuaries: controls and ecophysiological and ecosystem consequences. Limnol Oceanogr 42:1105–1118

van der Heijden LH, Kamenos NA (2015) Reviews and syntheses: calculating the global contribution of coralline algae to total carbon burial. Biogeosciences 12: 6429–6441

Walvoord MA, Striegl RG (2007) Increased groundwater to stream discharge from permafrost thawing in the Yukon River basin: potential impacts on lateral export of carbon and nitrogen. Geophys Res Lett 34:L12402

Woelkerling WJ, Irvine LM, Harvey AS (1993) Growth-forms in non-geniculate coralline red algae (Coralliinales, Rhodophyta). Aust Syst Bot 6:277–293

Worm B, Reusch TBH, Lotze HK (2000) *In situ* nutrient enrichment: methods for marine benthic ecology. Int Rev Hydrobiol 85:359–375

Zuur AF, Ieno EN, Walker NJ, Saveliev AA, Smith GM (eds) (2009) Mixed effects models and extensions in ecology with R. SpringerLink (online service), New York, NY

Editorial responsibility: Morten Pedersen, Roskilde, Denmark

Submitted: November 6, 2019; Accepted: March 25, 2020
Proofs received from author(s): May 23, 2020